PCCP

PAPER

The *Crystal-T* algorithm: a new approach to calculate the SLE of lipidic mixtures presenting solid solutions†

Guilherme J. Maximo,[a] Mariana C. Costa[b] and Antonio J. A. Meirelles*[a]

Lipidic mixtures present a particular phase change profile highly affected by their unique crystalline structure. However, classical solid–liquid equilibrium (SLE) thermodynamic modeling approaches, which assume the solid phase to be a pure component, sometimes fail in the correct description of the phase behavior. In addition, their inability increases with the complexity of the system. To overcome some of these problems, this study describes a new procedure to depict the SLE of fatty binary mixtures presenting solid solutions, namely the "*Crystal-T* algorithm". Considering the non-ideality of both liquid and solid phases, this algorithm is aimed at the determination of the temperature in which the first and last crystal of the mixture melts. The evaluation is focused on experimental data measured and reported in this work for systems composed of triacylglycerols and fatty alcohols. The *liquidus* and *solidus* lines of the SLE phase diagrams were described by using excess Gibbs energy based equations, and the group contribution UNIFAC model for the calculation of the activity coefficients of both liquid and solid phases. Very low deviations of theoretical and experimental data evidenced the strength of the algorithm, contributing to the enlargement of the scope of the SLE modeling.

[a] *Laboratory of Extraction, Applied Thermodynamics and Equilibrium, School of Food Engineering, University of Campinas, R. Monteiro Lobato 80, 13083-862, Campinas, São Paulo, Brazil. E-mail: tomze@fea.unicamp.br; Fax: +55 19 3521 4027; Tel: +55 19 3521 4037*

[b] *School of Applied Sciences, University of Campinas, R. Pedro Zaccaria, 1300, 13484-350, Limeira, São Paulo, Brazil. E-mail: mariana.costa@fca.unicamp.br; Fax: +55 19 3701 6680; Tel: +55 19 3701 6673*

† Electronic supplementary information (ESI) available: Description of the SLE equations, tables with pure components melting properties and mixtures' experimental SLE data and Tammann plots of the eutectic transitions. See DOI: 10.1039/c4cp01529k

Introduction

Several studies in the literature report the understanding of the melting and crystallization phenomena of systems formulated by lipidic compounds as well as the modeling of their solid–liquid equilibrium (SLE) behaviour.[1–7] However, the more complex the systems are, the harder it is to understand and model their melting profile. Fats and oils mixtures are known to present particular crystalline structures, which are highly dependent on the processes and conditions to which the mixtures are exposed. A common phenomenon in this context is the formation of solid solutions, in which crystals of a compound are fitted into the lattice of another crystal.[8] Lipid-based products commonly exhibit this phenomenon, highly affecting the rheological and physicochemical profile of the system.[9,10]

Mixtures of triacylglycerols and fatty alcohols, evaluated here, are an example. Fatty alcohols are used as surfactant structuring agents in lipid-based systems for the replacement of hydrogenated vegetable oils or saturated TAGs. Moreover, TAGs and fatty alcohols are used in microbiostatic coatings for foods, formulation of organogels or controlled release medicines.[11–17]

Phase equilibrium modeling is the ideal first step for the optimization and design of industrial operations as well as the formulation of products with desired properties. However, usual approaches presented in literature fail to describe the SLE behavior of lipidic mixtures either by the lack of the experimental properties of pure compounds or by describing them as simple eutectic systems and consequently neglecting the presence of solid solutions. In fact, a few studies have used approaches to model the SLE of fatty mixtures taking into account the presence of solid solutions,[2,18,19] but none of them present a complete description of the non-ideal behavior of both liquid and solid phases. In addition, they use computational routines that can be very sensitive to initial estimates. For this reason, this work was aimed at describing a robust and effective procedure to calculate the SLE of binary fatty systems presenting solid solutions, namely the *Crystal-T* algorithm. To evaluate the effectiveness of the algorithm, binary systems composed of triacylglycerols (TAGs) and fatty alcohols were experimentally determined by differential scanning calorimetry and microscopy, and then modeled by this new approach.

These systems were chosen because of the formation of a significant solid solution region depending on the concentration of the compounds.

The procedure proposed by the *Crystal-T* algorithm for the calculation of the SLE point was based on the classical "*Bubble-T*" algorithm[20–23] used for the determination of the *bubble point* in the vapor–liquid equilibrium (VLE) calculation. The great novelty proposed by this routine is that it considers the non-ideality of both liquid and solid phases by the classical isofugacity equilibrium thermodynamic criteria and activity coefficient models to calculate the *liquidus* and *solidus* lines of the phase diagrams. Moreover, it uses information obtained by the Tammann plots of the eutectic transition to describe the solid solution region of the diagram. The set of non-linear equations that characterize the problem described by the *Crystal-T* algorithm was solved by an optimization routine that identifies the temperatures at which the first and last crystals melt for a mixture with a known composition.

Theory

Fundamentals

Considering an isobaric system, the classical thermodynamics establish a well-defined theory for the description of the solid–liquid equilibrium (SLE) relating 3 fundamental variables: the mole fraction of the compound i in the liquid phase x_i, in the solid phase, z_i and temperature T. The equation that relates these variables is built through the isofugacity criteria.[21–23] Taking into account the relation between the fugacities of the compounds in both the phases, the SLE is described by the calculation of the Gibbs energy of a defined heating-cooling process, depicted in Fig. 1. Further details are in the ESI.† The SLE is expressed by eqn (1).

$$\ln \frac{x_i \gamma_i^L}{z_i \gamma_i^S} = \frac{\Delta_{fus}H}{R}\left(\frac{1}{T_{fus}} - \frac{1}{T}\right) + \sum_{tr=1}^{n}\left[\frac{\Delta_{tr}H}{R}\left(\frac{1}{T_{tr}} - \frac{1}{T}\right)\right]$$
$$+ \frac{\Delta_{fus}C_p}{R}\left(\frac{T_{fus}}{T} - \ln\frac{T_{fus}}{T} - 1\right) \quad (1)$$

where γ_i^L and γ_i^S are the activity coefficients of the component i in the liquid and solid phases, respectively, T is the melting temperature (K) of the mixture, R is the ideal gas constant
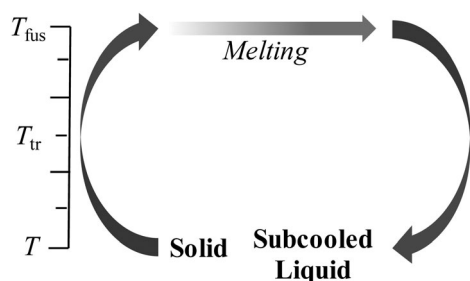
(8.314 J mol^{-1} K^{-1}), T_{fus} and $\Delta_{fus}H$ are the melting temperature (K) and enthalpy (J mol^{-1}) of the component i, T_{tr} and $\Delta_{tr}H$ are thermal transitions temperatures (K) and enthalpies (J mol^{-1}) of the n solid–solid transition (polymorphic forms) of the component i, respectively, and $\Delta_{fus}C_p$ is the difference between the heat capacity (J mol^{-1} K^{-1}) of the pure component i of the liquid and solid phases.

To describe the SLE of a mixture, T, x_i and z_i must be calculated by eqn (1), and the adjustment of the γ_i equations. This is classically obtained by a numerical optimization procedure. However, considering the high non-linearity of eqn (1), some theoretical approximations, well-applied for simplest cases, are frequently found in literature. The general suppositions are that (i) the specific heat capacity of the pure compounds can be neglected when compared with the magnitude of the $\Delta_{fus}H$; (ii) the compounds in the solid phase are immiscible such that the term related to the non-ideality of the component i in the solid phase is $z_i\gamma_i^S = 1.0$; and (iii) the liquid phase behaves as in an ideal system with the liquid phase activity coefficient $\gamma_i^L = 1.0$. In addition, although solid–solid (polymorphic) transitions of the pure compounds are often neglected, when compared to the $\Delta_{fus}H$ values, the magnitude of the $\Delta_{tr}H$ can significantly impact the modeling results. Despite the eventual non reliability of one of these hypotheses, the intrinsic nature of the adjustment can generate good results. Consequently, all these assumptions must be carefully evaluated.

A marked feature of the SLE of fatty mixtures is the appearance of solid solutions. From the SLE point of view, solid solutions are so that $z_i\gamma_i^S \neq 1.0$. Therefore, the activity coefficients of the component i in both the liquid γ_i^L and solid phase γ_i^S should necessarily be taken into account. In this work, the well-known Margules equation was used for the calculation of both γ_i^L and γ_i^S models as well as the group contribution UNIFAC equation for the description of γ_i^L. The Margules equation is a function relating T, x_i or z_i that can accurately model systems comprising chemicals with similar molar volumes.[21] In the case of binary mixtures, this equation can be written using one or two adjustable parameters, namely the 2- or 3-suffix Margules equations, eqn (2) and (3) by considering the utilization of up to quadratic or cubic terms[21] can be expressed as follows:

$$\gamma_i = \exp\left(\frac{A_{ij}z_j^2}{RT}\right) \quad (2)$$

$$\begin{cases} \gamma_i = \exp\left[\frac{(A_{ij} + 3B_{ij})z_j^2 - 4B_{ij}z_j^3}{RT}\right] \\ \gamma_j = \exp\left[\frac{(A_{ij} - 3B_{ij})z_i^2 + 4B_{ij}z_i^3}{RT}\right] \end{cases} \quad (3)$$

where i, j = components 1, 2 and A_{ij} and B_{ij} (kJ mol^{-1}) are the empirical parameters related to the thermodynamic interactions between the two compounds in the mixture. The UNIFAC (UNIQUAC Functional-group Activity Coefficient) model is a predictive model based on the group-contribution concept[24,25] in which the activity coefficient can be found by the sum of both the enthalpic and entropic contributions of the chemical

Fig. 1 Thermodynamic cycle comprising the heating, melting and cooling processes of the system, from T to T_{fus}, from a solid to a subcooled liquid state taking into account the polymorphism phenomena at T_{tr}.

groups in the mixture. Some modifications of this model consider the temperature-dependence of the enthalpic contribution or changes in the entropic contribution.[26] Details concerning the UNIFAC model are described elsewhere.[24–26] Thus, in this work, the following approaches were used for calculating the activity coefficients: (i) original UNIFAC or UNIFAC-Dortmund models for γ_i^L and 2-suffix Margules equation for γ_i^S; (ii) original UNIFAC model for γ_i^L and 3-suffix Margules equation for γ_i^S; (iii) 2-suffix Margules equation for both γ_i^L and γ_i^S; and (iv) 3-suffix Margules equation for both γ_i^L and γ_i^S. In the case of UNIFAC models, the parameters were taken from literature.[26,27]

Considering the non-ideality of the solid phase ($z_i\gamma_i^S \neq 1.0$), the system can present as either continuous or discontinuous solid solutions. In this work, the evaluated mixtures present discontinuous solid solutions, in which the compounds are miscible in the solid phase in a restrained concentration range. This case is analogous to the VLE of azeotropy-heterogeneous mixtures. The classical shape of this phase diagram is shown in Fig. 2. The curves that circumscribe the biphasic region are called *liquidus* and *solidus* lines and describe the melting temperature T of the mixture as a function of x_i and z_i, respectively. At $T = T_{eut}$, the behavior of both the curves presents a discontinuity. This is because of the formation of an additional solid phase, establishing a solid–solid–liquid equilibrium state. According to the isofugacity criteria, this triphasic point is such that

$$x_i\gamma_i^L f_i^{L^0} = \left(z_i\gamma_i^S f_i^{S^0}\right)_I = \left(z_i\gamma_i^S f_i^{S^0}\right)_{II} \qquad (4)$$

where $f_i^{L^0}$ and $f_i^{S^0}$ are the standard state fugacities of the compound i in the liquid phase and in both the solid phases I and II. This point is the so-called eutectic point, in which the mixture at a composition x_i, z_i^I, z_i^{II} melts at a minimum and single temperature T_{eut}. From an industrial point of view, the correct determination of the eutectic point is of utmost importance if one is interested in the formulation of mixtures with low melting points, for instance to avoid solidification at low temperatures,
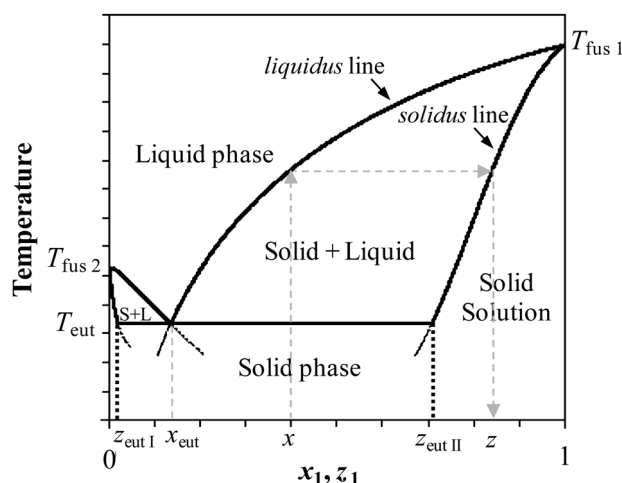

Fig. 2 Solid–liquid equilibrium phase diagram of a discontinuous binary solid solution case.

as in the case of biodiesel mixtures,[28–30] lubricants or controlled melting mixtures.[31,32]

SLE algorithms

The equilibrium thermodynamic theory is well established for the resolution of the vapor–liquid and liquid–liquid equilibria. On the other hand, the SLE problems have been developed by analogies using the same models for the description of the non-ideality of the phases. Two algorithms have been already presented in the literature for the description of SLE: the stability test based on the Gibbs energy minimization and the isoenthalpic *flash* calculation. Both are explained in detail elsewhere.[2,18,19,33]

In the first case, the algorithm considers that for a given temperature or composition, a system at equilibrium has the minimum Gibbs energy G. The function that represents G is written by relating the activity coefficients of the phases γ_i^L and γ_i^S, as described in eqn (5).

$$G = n^L g^L + n^S g^S = g^L = n^L RT \sum_{i=1}^{nc} x_i \ln\left(x_i\gamma_i^L\right)$$

$$+ n^S RT \sum_{i=1}^{nc} z_i \left\{ \frac{\Delta_{fus}H}{R}\left(\frac{1}{T_{fus}} - \frac{1}{T}\right) + \sum_{tr=1}^{n}\left[\frac{\Delta_{tr}H}{R}\left(\frac{1}{T_{tr}} - \frac{1}{T}\right)\right] \right.$$

$$\left. + \frac{\Delta_{fus}C_p}{R}\left(\frac{T_{fus}}{T} - \ln\frac{T_{fus}}{T} - 1\right) + \ln z_i\gamma_i^S \right\} \qquad (5)$$

where n^L, n^S, g^L and g^S are the number of moles n and the mole Gibbs energy g of both the liquid L and solid S phases, respectively. Mathematically, the minimum of eqn (5) is obtained by an optimization procedure in which using a defined mixture at a fixed temperature T the composition of the system in the equilibrium condition is obtained. Considering a binary mixture this problem becomes bidimensional and the independent variables could be the number of moles of the liquid phase n_i^L. The number of moles of the solid phase n_i^S is calculated by the mass balance of the system.

In the case of the isoenthalpic *flash* calculation, the algorithm considers that a system with a known composition feeds a vessel at a fixed temperature T and pressure P where the equilibrium condition must be satisfied. The final composition is calculated by equations relating mass balances as well as the SLE equilibrium equation (eqn (1)). The solution is based on the minimization of an objective function written by this set of equations, of which the most known equations are the Rachford and Rice equation (eqn (6)), as presented elsewhere.[20,34]

$$\sum_{i=1}^{2} x_i - \sum_{i=1}^{2} z_i = \sum_{i=1}^{2} \frac{(K_i - 1)n_i}{1 + \beta(K_i - 1)} = 0 \qquad (6)$$

where K_i is the x_i/z_i ratio obtained from eqn (1), n_i is the number of the moles of the compound i in the feeding and β is the ratio between the liquid phase amount L and the total feed mixture F.

In this work, to evaluate the effectiveness of the proposed *Crystal-T* algorithm, the Gibbs and *flash* algorithms were implemented for the description of the SLE phase diagrams

of the binary fatty systems. The minimization of the free Gibbs energy was written using a procedure based on a multidirectional optimization problem. In this case, a sequential quadratic problem (SQP) algorithm was used given by the MATLAB function *fmincon*. The isoenthalpic *flash* calculation algorithm was implemented using an optimization routine written in LINGO (Lindo Systems) for the minimization of the Rachford and Rice equation (eqn (6)). For this, a generalized reduced gradient (GRG) method for non-linear problems was considered. Markedly, both the algorithms are highly dependent on the initial estimate because it must be within the biphasic domain for the complete description of the *liquidus* and *solidus* lines of the SLE diagram. Once the biphasic domain is unknown, the introduction of additional algorithms to test the initial estimate or the number of phases in the equilibrium state becomes necessary.

The *Crystal-T* algorithm

The *Crystal-T* algorithm is aimed at the construction of the *liquidus* and *solidus* lines of the SLE phase diagram, as shown in Fig. 1, which represents temperature T as a function of x_i and z_i. The procedure was based on the classical "*Bubble-T*" algorithm, which is used for the calculation of vapor–liquid equilibrium. Using VLE thermodynamic equations and the classical γ–ϕ approach, the "*Bubble-T*" algorithm calculates the temperature and composition of the vapour phase in which the "last bubble" of the mixture is formed in the equilibrium state for a given liquid phase and pressure. The algorithm is similar to that presented in Fig. 3, and is used in this work. However, two main considerations

must be addressed. The first one is the proper transposition for the solid–liquid case with the utilization of SLE equations and, consequently the utilization of γ equations for both the solid and liquid phases. The second is that the "*Bubble-T*" algorithm does not consider the cases with triphasic equilibrium conditions, as presented in Fig. 2. Using experimental data provided by the Tammann plots, this problem is overcome by a simple and effective approach, as will be explained in detail.

First, the routine to determine SLE condition was formulated so that the mole fraction of the compound i in the solid phase z_i and the melting temperature T are calculated to answer the equilibrium criteria (eqn (1)) for a given mole fraction of the compound i in the liquid phase x_i. The procedure was based on finding the root of the function F, which is defined as the mole balance of the solid phase (eqn (7)).

$$F = \left| 1 - \sum_i^2 z_i \right| \tag{7}$$

where,

$$z_i = \exp\left[\ln \frac{x_i \gamma_i^L}{\gamma_i^S} - \frac{\Delta_{fus}H}{R}\left(\frac{1}{T_{fus}} - \frac{1}{T} \right) \right.$$
$$\left. - \sum_{tr=1}^n \left[\frac{\Delta_{tr}H}{R}\left(\frac{1}{T_{tr}} - \frac{1}{T} \right) \right] - \frac{\Delta_{fus}C_p}{R}\left(\frac{T_{fus}}{T} - \ln\frac{T_{fus}}{T} - 1 \right) \right] \tag{8}$$

$$\gamma_i^L = f(x_i, T, \text{parameters of the equation}) \tag{9}$$

$$\gamma_i^S = f(z_i, T, \text{parameters of the equation}) \tag{10}$$

$$0.0 < x_i, z_i < 1.0 \ (x_i, z_i \in \Re; \ i = 1, 2) \tag{11}$$

$$T > 0.0 \ (T \in \Re) \tag{12}$$

Fig. 3 shows the block diagram of the routine. (1) The algorithm starts for a given composition x_i, a set of phase transition properties T_{fus}, $\Delta_{fus}H$, T_{tr}, $\Delta_{tr}H$, $\Delta_{fus}C_p$ and parameters for the γ_i equations. The parameters are A_{ij} (J mol^{-1}) in the case of the 2-suffix Margules equation, A_{ij} and B_{ij} (J mol^{-1}) in case of the 3-suffix Margules equation and for the UNIFAC model, the structural parameters for each group k, R_k and Q_k, and the group-interaction parameters a_{mn} between the groups m and n in the mixture. A melting temperature T is first assumed and γ_i^S taken as 1.00. (2) In the first interaction, z_i is calculated (eqn (8)), the solid phase mole fractions are normalized and the γ_i^S calculated considering the estimated T and the new z_i values. (3) In the following step, Σz_i is newly calculated (eqn (8)) and compared with the previous one with a tolerance level lower than 1×10^{-4}. Once such a comparison is made, (4) the mole balance of the solid phase is tested with the same tolerance level. The values for T and z are then obtained if such a criterion is established. If the criterion is not satisfied, (5) a new estimate for $T(T^*)$ is done through a modified quasi-Newton method in which only the first derivative of the function F is considered (eqn (13)). The numerical derivative of the function F' was calculated by an infinitesimal range of $\delta T = 5 \times 10^{-3}$. The convergence is established at a

Fig. 3 Block diagram of the main algorithm for the calculation of the SLE point.

tolerance level lower than 1×10^{-5} (the tolerance levels established in the routine were chosen to be sufficient to express the variables T and z_i with the desired accuracy, enabling faster convergence). The new T^* value is then used in the next iteration.

$$T^* = T + \frac{F}{F'} \tag{13}$$

Because the eutectic transition establishes a minimum point in the *liquidus* and *solidus* lines, in the domain restrained by $T_{\text{fus}} < T < T_{\text{eut}}$, with T_{fus} being the lower melting temperature between both the pure compounds, there are two composition pairs (x_i, z_i) satisfying the equilibrium criteria for one single temperature T. Thus, a well approximated estimate for T in the procedure is required. For this reason, the algorithm is calculated for $0.0 < x_i < 1.0$ and sequentially for $1.0 < x_i < 0.0$. The first calculation starts at $T = T_{\text{fus},2}$ and the second one at $T = T_{\text{fus},1}$. At each iteration, the initial estimate for T is given by the melting temperature of the previous iteration and the composition step $\delta x_i \leq 0.01$. This procedure led to the appearance of two profiles T, x_i, z_i, as depicted in Fig. 2 with the interception of the curves of the solid–solid–liquid equilibrium state (eqn (4)) corresponding to the eutectic point. The supposed extension of the melting behavior of each profile is depicted by dashed lines in Fig. 2. They are metastable melting transitions possibly present in the heating process of the mixture. The extensions of the lines were, consequently, neglected to depict the phase diagram. It is remarkable that in the case of no discontinuity in the behavior of the functions, the algorithm naturally satisfies the continuous solid solution case with no further procedures, whether comprising minimum/maximum points or not.

Adjustment of the γ_i equation parameters

Once the algorithm for the calculation of the SLE was established, the parameters of the 2- and 3-suffix Margules equations were adjusted using an optimization routine that embodies the main algorithm, as presented in Fig. 3. Considering the calculation of γ_i^{L} and γ_i^{S}, one, two or four parameters were fitted depending on the approach used. In this work, the adjustment of one parameter, for using the UNIFAC model and 2-suffix Margules equation for γ_i^{L} and γ_i^{S} calculation, respectively, was implemented using an algorithm based on the Nelder–Mead Simplex direct search (MATLAB function *fminsearch*). The objective function used in this procedure was built, as proposed by literature,[35] taking into account the ratio between the square absolute deviations between the calculated and experimental (*exp.*) data and the experimental uncertainties σ^2, as follows:

$$\delta = \left(\sum_i^n \frac{|T_i - T_i^{\text{exp}}|^2}{\sigma_{T_i^{\text{exp}}}^2} \right) + \frac{|T_{\text{eut}} - T_{\text{eut}}^{\text{exp}}|^2}{\sigma_{T_{\text{eut}}^{\text{exp}}}^2} + \frac{|x_{\text{eut}} - x_{\text{eut}}^{\text{exp}}|^2}{\sigma_{x_{\text{eut}}^{\text{exp}}}^2}$$
$$+ \frac{|z_{\text{eut}} - z_{\text{eut}}^{\text{exp}}|_{\text{I}}^2}{\sigma_{z_{\text{eut}_{\text{I}}}^{\text{exp}}}^2} + \frac{|z_{\text{eut}} - z_{\text{eut}}^{\text{exp}}|_{\text{II}}^2}{\sigma_{z_{\text{eut}_{\text{II}}}^{\text{exp}}}^2} \tag{14}$$

where T_i are the mixture melting temperature and $(T, x_i, z_i^{\text{I}}, z_i^{\text{II}})_{\text{eut}}$ represents the eutectic point, *i.e.* the solid–solid–liquid equilibrium SSLE point with two solid phases I and II. The experimental

eutectic point was calculated using the well-known Tammann plot by the evaluation of the behavior of the eutectic enthalpies as a function of the concentration, as explained elsewhere.[36–38] The uncertainties were obtained experimentally, as discussed later.

In the adjustment of two parameters, for using the UNIFAC model and 3-suffix Margules equation for γ_i^{L} and γ_i^{S} calculation, respectively or using the 2-suffix Margules equation for the calculation of both γ_i^{L} and γ_i^{S} and in the adjustment of four parameters by using the 3-suffix Margules equation for both phases, the numerical optimization fails to find a unique solution. It implies that not a single set of adjustable parameter can answer an optimization routine. This problem is well-known in the literature[21,35] for the calculation of non-linear thermodynamic problems. By determining both *liquidus* and *solidus* lines, the number of the independent variables increases when compared with the description of only the *liquidus* line and the number of adjustable parameters. Considering that the number of experimental data points is the same, the degrees of freedom of the problem also increase. This prevents from obtaining a unique solution. For this reason, a heuristic method was adopted. The problem is finding the set of parameters A_{ij} and B_{ij} of the 2- and/or 3-suffix Margules equation (eqn (2) and (3)) that minimizes the deviation between the calculated and experimental data (eqn (14)). Considering n number of parameters to adjust, depending on the case, n vectors with m elements were built. The m elements were the possible solutions for the problem. Thus, $n \times m$ sets of calculated data were found and the deviation (eqn (14)) was calculated for each set. A multi-dimensional surface relating the $n \times m$ sets of parameters and the deviation were then observed. The surface presented a minimum region that circumscribed the set of parameters and answered the problem.

The overall modeling procedure can be summarized by Fig. 4. The routine is represented by a three level nested structure: (1) the first one is the main algorithm where the equilibrium point (T, x_i, z_i) is calculated; (2) the second one comprises the execution of the first level for $0.0 < x_i < 1.0$ and sequentially for $1.0 < x_i < 0.0$ to depict the SLE phase diagram; (3) the third one is the adjustment of the γ_i parameters by a numerical or a heuristic optimization procedure in which the first and the second levels are executed until convergence is established.
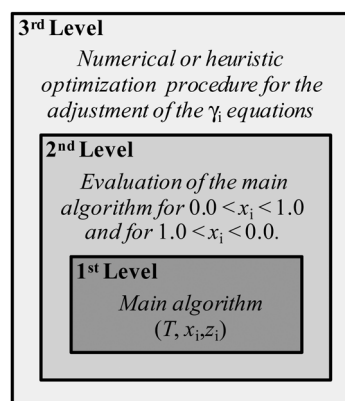

Fig. 4 Nested structure for the *Crystal-T* algorithm.

16744 | *Phys. Chem. Chem. Phys.*, 2014, **16**, 16740–16754

This journal is © the Owner Societies 2014

Experimental considerations

The *Crystal-T* algorithm was used in the modeling of SLE experimental data of the following triacylglycerol + fatty alcohol mixtures: trilaurin + 1-hexadecanol, trilaurin + 1-octadecanol, trimyristin + 1-hexadecanol, trimyristin + 1-octadecanol, tripalmitin + 1-hexadecanol and tripalmitin + 1-octadecanol. As previously specified, the SLE problem takes into account the knowledge of the transition properties of pure compounds. In this work, specific heat capacity $\Delta_{fus}C_p$, solid–solid transition temperature T_{tr} and enthalpy $\Delta_{tr}H$ were taken from literature.[2,39–42] Melting temperatures T_{fus} and enthalpies $\Delta_{fus}H$ of the pure triacylglycerols and fatty alcohols (Sigma-Aldrich, 99% mass fraction) were obtained by six-replicates using differential scanning calorimetry with a DSC8500 calorimeter (PerkinElmer, Waltham) at ambient pressure following a specific methodology developed for fatty systems, as described elsewhere.[36,38] The melting temperatures and enthalpies of the pure compounds were compared with literature values,[2,39,40,42–48] and low mean relative deviations of 1.1% and 5.5%, respectively, were observed. The triacylglycerol + fatty alcohol mixtures were prepared gravimetrically and their melting properties were obtained following the same methodology.

Because at the beginning of the melting process (*solidus* line), in the case of solid solution formation is difficult to identify by using DSC data, which is often overestimated, the mixtures were evaluated by temperature controlled microscopy using a BX51 Olympus optical microscope (Olympus Co., Tokyo) coupled to a LTS120 Linkam temperature-controller apparatus (Linkam Scientific Instruments Ltd, Tadworth). Samples were cooled at a rate of 0.5 K min^{-1}, and observed in a 0.1 K min^{-1} heating run. Melting temperatures of the pure compounds and some of their mixtures were evaluated by microscopy and the results were compared with the DSC data. Deviations between experimental data obtained by DSC and by microscopy were estimated to be not higher than 1.0 K.

The uncertainty of the melting temperature of the mixture was obtained by the evaluation of at least three replicates of the pure compounds and some of the binary mixtures. The uncertainty of the eutectic point was calculated by error propagation method, considering the equations obtained in the fitting procedure of the Tammann plot. The x_i experimental errors were also calculated by error propagation from the values of the weighted masses. Uncertainties for melting temperatures and mole fractions as well as for eutectic temperature and mole fraction were estimated as not higher than ± 0.38 K, ± 0.001, ± 0.58 K and ± 0.005, respectively.

Because the evaluation of the SLE experimental data is fundamental for the accuracy of the modeling procedure, their results will be explained in detail.

Results and discussion

Experimental data analysis

Fig. 5 depicts the solid–liquid transition experimental data of the binary mixtures as well as the modeled *liquidus* and *solidus* lines. Tables with experimental data are reported in the ESI.† The DSC technique was able to clearly show the melting temperature behavior of the mixtures, *i.e.* the *liquidus* line and the eutectic reaction when it exists. Fig. 6 shows the melting behavior observed by the DSC thermograms obtained for the trimyristin (1) + 1-hexadecanol (2) mixture. In all the cases, the *liquidus* line shows a minimum and an invariant transition is observed at the same temperature of this inflexion point. This behavior is typically observed in the case of systems presenting eutectic transitions.

The eutectic transition and the formation of solid solution were investigated using Tammann plots and temperature-controlled microscopy. Fig. 7 presents the Tammann plots of the trimyristin (1) + 1-hexadecanol (2) mixture for the observed invariant transition, and Fig. 8 shows the optical micrographs for the melting process of the same mixture at $x_1 = 0.694$ mole fraction. At this concentration, DSC data show the presence of an invariant transition at $T = 319.46$ K. Micrographs obtained at temperatures before and after $T = 319.46$ K show that at this temperature the mixture clearly starts to melt, delimiting the biphasic region. In fact, the well-described triangular-shape of the Tammann plot of the invariant transition, considering the linear regressions of the data ($R^2 > 0.98$), was able to show the typical profile of a eutectic transition. It implies that the enthalpy of the transition increases up to the eutectic point ($x_1 = 0.124 \pm 0.005$ mole fraction) when it begins to decrease.

Note that enthalpy associated with the eutectic transition disappears at $x_1 = 0.0$ mole fraction in the left-hand side of the Tammann plot and at $x_1 = (0.775 \pm 0.005)$ mole fraction in the right-hand side. It implies that in case of the trimyristin (1) + 1-hexadecanol (2) mixture at the left-hand side of the phase diagram the solid phase in the biphasic region is composed of pure fatty alcohol or, considering the experimental uncertainty, a solid solution with a composition very close to pure fatty alcohol. However, in the right-hand side of the diagram, the system is a mixture with both the compounds in the solid-phase as a solid solution ($x_1 \geq 0.775$ mole fraction). For other mixtures, solid phase miscibility was also observed at the triacylglycerol-side of the diagram. The Tammann plots for all the systems are provided in ESI.† In summary, trilaurin (1) + 1-hexadecanol (2) presents a eutectic at $(x_1, z_1^I, z_1^{II}) \cong (0.552, 0.000, 0.949)$ mole fraction, trimyristin (1) + 1-octadecanol (2) at $(x_1, z_1^I, z_1^{II}) \cong (0.521, 0.000, 0.937)$ mole fraction, tripalmitin (1) + 1-hexadecanol (2) at $(x_1, z_1^I, z_1^{II}) \cong (0.025, 0.000, 0.743)$ mole fraction and tripalmitin (1) + 1-octadecanol (2) at $(x_1, z_1^I, z_1^{II}) \cong (0.112, 0.000, 0.682)$ mole fraction. Thus, at $x_1 > x_{eut}$, the solid phase of the mixture is composed of both the compounds at the biphasic domain. On the other hand, at $x_1 < x_{eut}$ experimentally it is virtually impossible to know if the solid phase of the system is really immiscible or if there is a small miscibility gap very close to pure fatty alcohol, *i.e.* $z_2 \cong 1.00$. The Tammann plot for trilaurin (1) + 1-octadecanol (2) shows an almost simple eutectic behavior with solid phase immiscibility in the entire concentration range. In this case, the eutectic point is at $(x_1, z_1^I, z_1^{II}) \cong (0.802, 0.000, 1.000)$ mole fraction. In summary, solid solutions are clearly seen in almost all the cases and
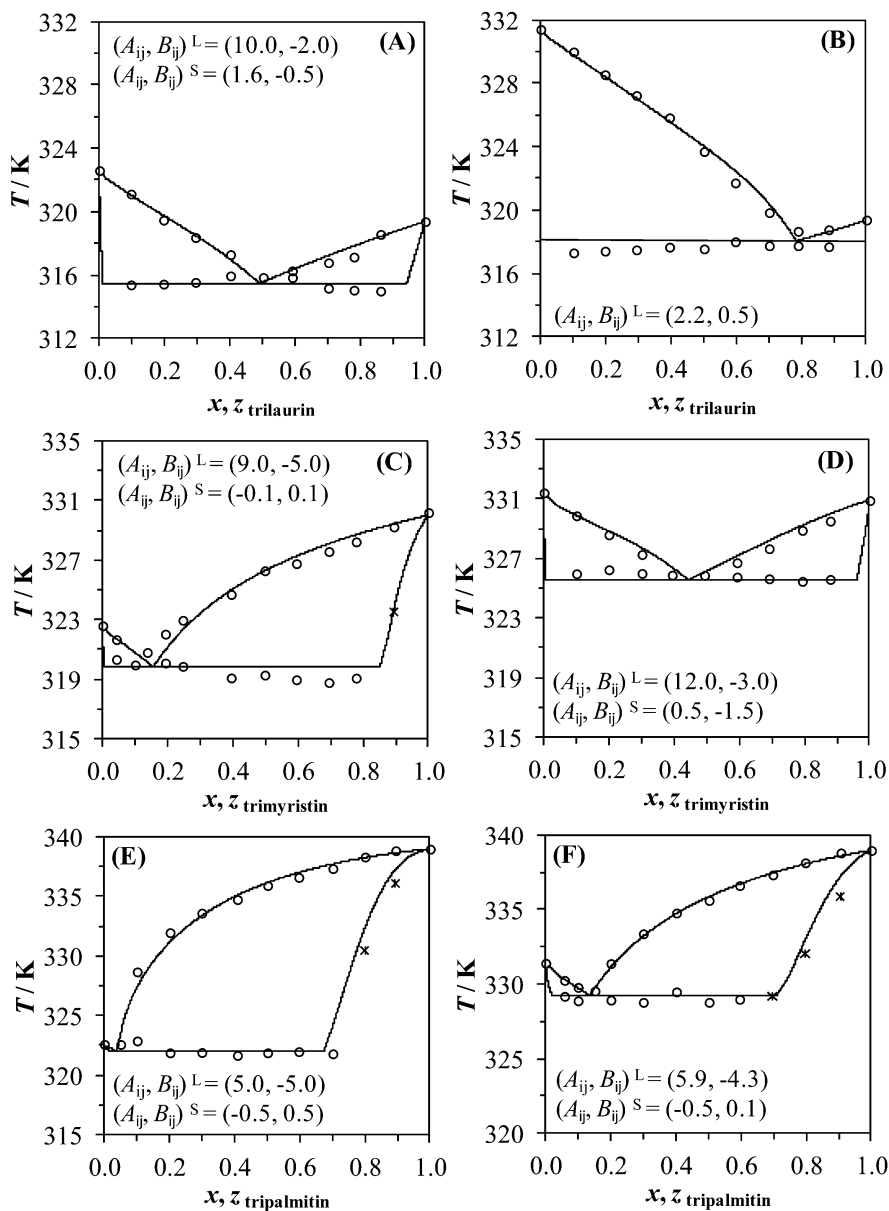
This journal is © the Owner Societies 2014

Phys. Chem. Chem. Phys., 2014, **16**, 16740–16754 | **16745**

Fig. 5 Experimental ($\bigcirc$ by DSC and * by microscopy) and modeled (solid lines) phase diagrams using the 3-suffix Margules equation for the triacylglycerol + fatty alcohols mixtures. A_{ij}^S, B_{ij}^S are the parameters for the γ_i^S equation and A_{ij}^L, B_{ij}^L for the γ_i^L equation (kJ mol^{-1}). (A) trilaurin (1) + 1-hexadecanol (2), (B) trilaurin (1) + 1-octadecanol (2), (C) trimyristin (1) + 1-hexadecanol (2), (D) trimyristin (1) + 1-octadecanol (2), (E) tripalmitin (1) + 1-hexadecanol (2), (F) tripalmitin (1) + 1-octadecanol (2).

always at the right-hand side of the diagram, indicating that they are triacylglycerol-rich solutions. In addition, the higher the difference between the melting temperature of the pure compounds or higher the triacylglycerol carbon chain, the larger is the solid solution region.

When the compounds in solid phase are miscible to form a solid solution, the transition for the description of the *solidus* line, *i.e.* when the first crystal melts, was difficult to observe by the DSC measurements (see highlights in Fig. 6). Thus, to first verify the previous supposition on the existence of solid solution and to indentify the temperature of the *solidus* line, the samples were also subjected to thermal-controlled

microscopy at this defined region. Fig. 9 shows the melting process of the trimyristin (1) + 1-hexadecanol (2) system at $x_1 = 0.894$ mole fraction beginning at a temperature $T < T_{eut}$. White arrows were used to highlight the appearance of the liquid phase at $T = 323.55$ K (Fig. 9D). A slight enlargement of the crystal is observed with the rounding of the angulated boundaries of the solid particle. Consequently, the amount of the liquid phase starts to increase on entering the biphasic region. This implies that the melting starts at a temperature higher than that previously evaluated as the eutectic transition ($T = 319.46$ K). Thus, at a temperature lower than $T = 323.55$ K only a solid solution exists.
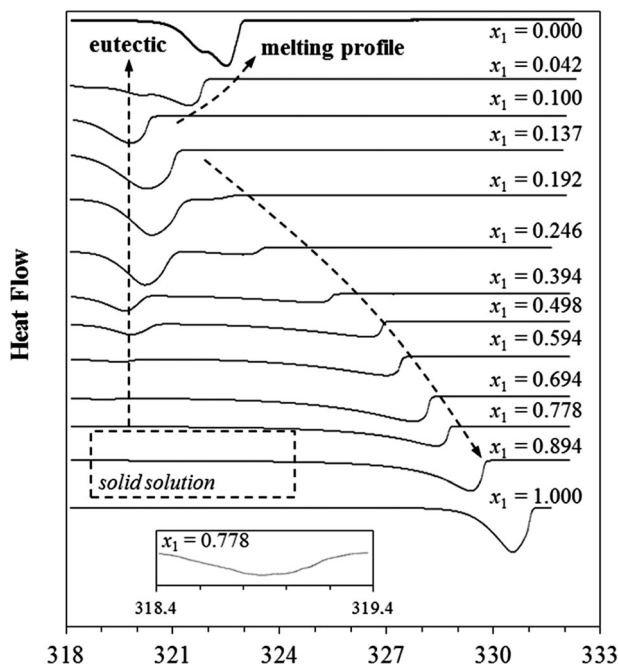
Fig. 6 Thermograms for the mixture trimyristin (1) + 1-hexadecanol (2). Magnification of the thermogram for $x_1 = 0.778$ mole fraction, in detail, showing the eutectic transition.
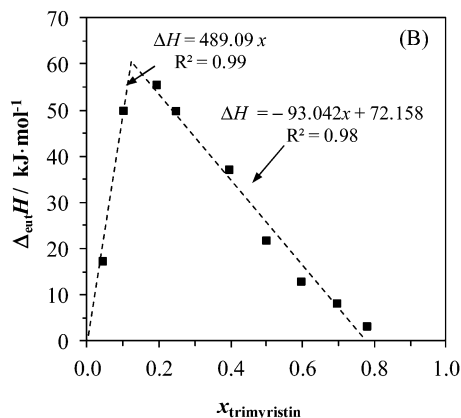

Fig. 7 Tammann plot of the enthalpy of eutectic transition for the trimyristin (1) + 1-hexadecanol (2) mixture. Dashed lines are linear regressions.

As previously mentioned, fatty compounds generally present some thermal transitions in the solid phase, and this is the case for both fatty alcohols and triacylglycerols. This phenomenon is well-known in the literature, and the compounds evaluated in this work have already been reported to present polymorphic forms during the heating of the solid phase.[2,36,39,48,49] All the triacylglycerols used in this work, trilaurin, trimyristin and tripalmitin present three principal polymorphic forms, namely α, β′ and β, with different crystal packing of hexagonal, orthorhombic and triclinic, respectively, and with increasing thermal stability and transition properties, temperatures and enthalpies. Apart from these principal polymorphic forms, some sub modifications in the crystal structure could occur during the heating

process, implying additional rearrangements of the long-carbon chains. Thus, a single thermogram may present several solid–solid transitions, related to these numerous conformational rearrangements of the crystal lattice of the compound. Fatty alcohols, specifically 1-hexadecanol and 1-octadecanol, investigated in this work, also present a characteristic polymorphic form whose transition temperature is very close to the melting temperature.[39,40] All these transitions are clearly evident in the thermograms of the pure compounds but are also present in the case of mixtures. The melting properties and the solid–solid of pure components –are presented in ESI.† Micrographs recorded before and after the solid–solid transition evidenced at $T = 318.75$ K for the system tripalmitin (1) + 1-octadecanol (2) at $x_1 = 0.697$ mole fraction are shown in Fig. 10. Changes in the crystalline structure of the mixture and in the refraction properties of the solid particle are clearly observed. This transition is probably related to one of the polymorphic forms of the tripalmitin because at the same temperature the pure compound presents a solid–solid transition that, according to literature,[2] is related to the α form ($T_{tr} = 317.85$ K). This thermal event is also identified by the thermogram of the mixture, as shown in Fig. 10. The thermogram clearly shows an endothermic transition followed by an exothermic one. This fact configures a resolidification phenomenon, which is probably related to a rearrangement to the β′ polymorphic form. The identification of the solid–solid transitions of the pure compounds is important because for transition temperatures higher than the eutectic point, the solid–liquid equilibrium behavior of the mixture is influenced by these transitions. This is described by eqn (1). Details regarding the SLE equation are presented in the ESI.†

SLE modeling using the *Crystal-T* algorithm

Taking into account the comprehension of the experimental melting behavior of the systems, modeling of the SLE phase diagrams was carried out. First, some remarks can be made considering the performance of the procedure. At the first level routine of the nested structure of the modeling procedure, (Fig. 4) the main algorithm was executed and the equilibrium point (T, x_i, z_i) of a mixture for a given liquid phase composition was calculated. Because the given liquid phase composition x_i lay on the *liquidus* line the equilibrium point could be directly determined and no additional routine to test the number of phases was required. On the other hand, using the Gibbs energy minimization and the isoenthalpic *flash* algorithms, the calculation of SLE was very sensitive to the initial estimate. If the composition was inside the biphasic region, the mixture is separated in two phases and the answer is the phase change point (T, x_i, z_i). However, out of this domain, the mixture has only one phase and the *liquidus* and *solidus* lines are not described, which require a routine to test the number of phases. Considering that the description of the entire SLE phase diagram implies the evaluation of a relatively large set of points that would be additionally followed by an adjustment for the γ_i models' parameters, numerical efforts increase exponentially. In addition to discussions on the performance of the procedures, the results obtained by the *Crystal-T*, the Gibbs or *flash* algorithms were
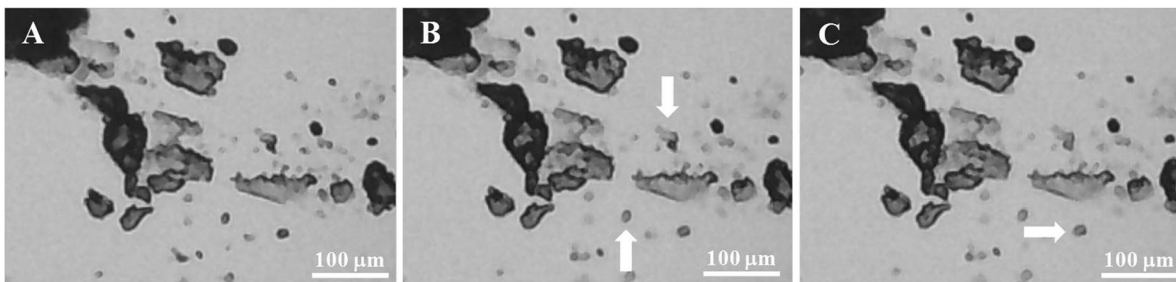
This journal is © the Owner Societies 2014

Phys. Chem. Chem. Phys., 2014, **16**, 16740–16754 | **16747**

Fig. 8 Melting transition at the eutectic temperature (T_{eut} = 319.46 K) for the trimyristin (1) + 1-hexadecanol (2) system at x_1 = 0.694 mole fraction. (A) 319.15 K, (B) 319.65, (C) 320.15 K. White arrows highlight the details during the melting process.
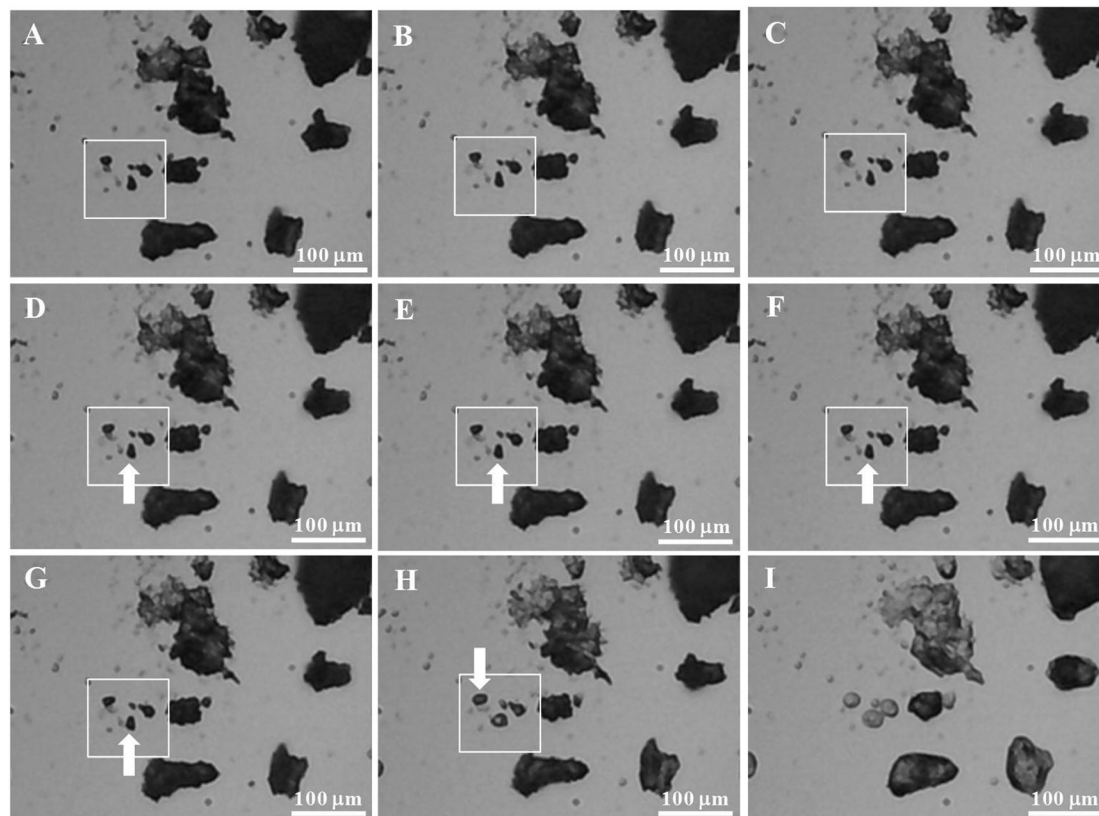

Fig. 9 Heating and melting processes of trimyristin (1) + 1-hexadecanol (2) system at x_1 = 0.894 mole fraction at T = (A) 313.15 K, (B) 322.15 K, (C) 323.35 K, (D) 323.55 K, (E) 323.95 K, (F) 324.35 K, (G) 325.40 K, (H) 327.65 K, and (I) 329.05 K. White arrows highlight the details during the heating process.

(and should be) exactly the same because they use the same thermodynamical theory expressed by eqn (1).

At the second level of the modeling, the main algorithm (Fig. 3) was executed considering each one of the pure compounds as initial estimate and generating two profiles with the interception of both profiles the solid–solid–liquid equilibrium point (Fig. 2). This procedure avoided additional phase test routines and problems with the discontinuity of the profile, as already mentioned.

At the third level of the procedure, the parameters of the liquid and solid γ_i equations were estimated. The results obtained were here exemplified by the system tripalmitin (1) + 1-octadecanol (2) because this case presented the larger solid solution region. For the estimation procedure, this work

considered that both the liquid and solid phases are non-ideal, and thus equations for depicting γ_i^L and γ_i^S were used. Two kinds of γ_i equations were evaluated. The UNIFAC model[24,26] is predictive, which is a great advantage for the design of a phase change based unitary operation if one does not know any experimental information about the mixture. On the other hand, the Margules equation is a function with adjustable parameters. Although such a model is not predictive, the function presents a lower non-linearity, reducing the numerical efforts but presenting a good agreement with the experimental data, as has been already reported in the literature.[38,50,51]

Fig. 11 depicts the SLE diagram of the system tripalmitin (1) + 1-octadecanol (2) using the original or modified UNIFAC
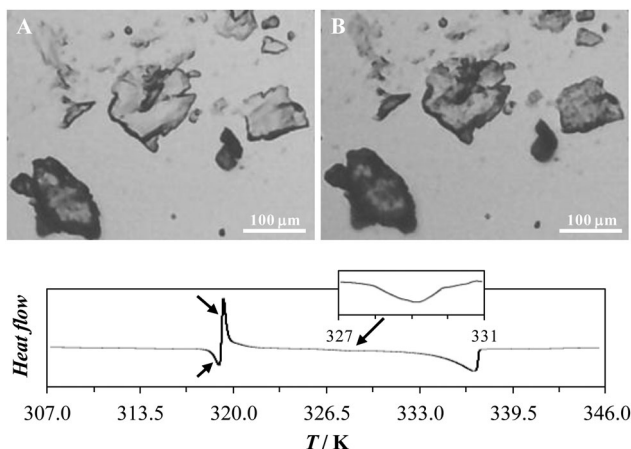
Fig. 10 Micrographs and thermogram of the system tripalmitin (1) + 1-octadecanol (2) at x_1 = 0.697 mole fraction. Pictures are at a temperature before ((A) 293.15 K) and after ((B) 320.15 K) the solid–solid transition at 318.75 K. Black arrows in the thermogram highlight the transitions. Eutectic transition in detail (T = 329.20 K).
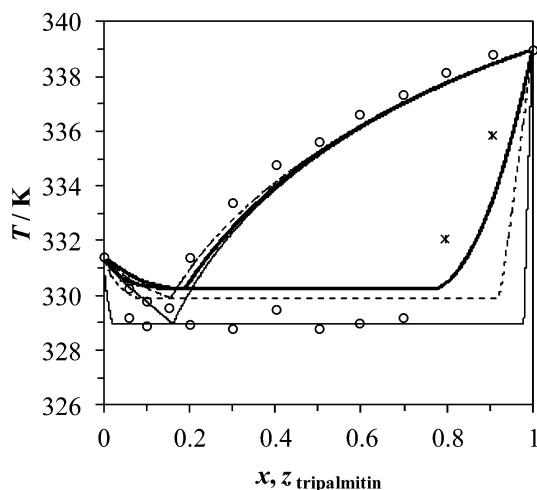

Fig. 11 SLE phase diagram of the tripalmitin (1) + 1-octadecanol (2) mixture using the 2-suffix Margules as γ_i^S equation and considering that γ_i^L = 1.0 (simple solid line) (A_{ij}^S = 6.93 kJ mol^{-1}) or using the original UNIFAC model (bold line) (A_{ij}^S = 6.23 kJ mol^{-1}) and the UNIFAC-Dortmund model (dashed line) (A_{ij}^S = 7.63 kJ mol^{-1}) as γ_i^L equation. DSC (○) and microscopy (*) data.

models to calculate the γ_i^L and the 2-suffix Margules equation to calculate the γ_i^S. In addition, the liquid phases were also considered to be ideal (γ_i^L = 1.0). In these cases, the optimization procedure is unidirectional, taking into account the adjustment of the A_{ij} parameter of the 2-suffix Margules equation.

These approaches fail in the prediction of the *liquidus* line as well as the SSLE (eutectic) temperature and composition. The γ_i^L values obtained from both the UNIFAC models did not deviate significantly from ideality. However, in the case of the original UNIFAC model, the solid phase positive deviation calculated by the 2-suffix Margules equation was slightly decreased when compared with the other approaches. The lower the positive

deviation from ideality, the lower the tendency of phase separation. Consequently, when the liquid phase was calculated by the original UNIFAC, the 2-suffix Margules described a *solidus* line with a solid solution domain larger than that described by the approach using the modified UNIFAC version. These observations show that probably neither the ideal assumption nor the UNIFAC models can accurately depict the liquid phase behavior or the 2-suffix Margules equation is not able to describe the solid phase non-ideality. Furthermore, the original and modified UNIFAC show different SLE profiles. If the original and modified UNIFAC models are compared, different combinatorial and residual terms are observed.[24,26] This implies that, considering the same system, both models can predict different molecular interactions and entropic effects. In fact, in some previous works[36,52] the original UNIFAC model was slightly more accurate in depicting the liquid phase behavior for the SLE of fatty systems than the modified version, despite modifications to improve the non-ideality calculation.

In addition, some works show that fatty compound molecules can be better represented by a different manner of counting groups, such as the ester group in TAG molecules, or using new or readjusted UNIFAC interaction parameters.[53,54] These considerations are allied to the fact that UNIFAC's parameters were adjusted by VLE experimental data,[24] showing that the utilization of the UNIFAC model for the accurate description of SLE is probably restricted to simple cases, such as that considering solid phase immiscibility. However, in this work, the use of the UNIFAC model for more complex approaches is also investigated. For this, and based on the aforementioned comments, the original version was chosen.

Using the 2-suffix Margules equation for the calculation of both phases' activity coefficients or the 3-suffix Margules equation and the original UNIFAC model for the calculation of γ_i^S and γ_i^L, respectively, the optimization procedure is bidirectional. Due to the set of experimental data points with an inherent experimental uncertainty as well as the number of parameters to fit the data, the problem could not be answered by numerical procedures and was solved by a heuristic method. For this, tridimensional surfaces were built relating the parameters used for the γ_i^L and γ_i^S calculation and the deviation (eqn (14)) generated by them. Fig. 12 and 13 show the contour plots of the surfaces generated by these approaches and sketch the changes in the calculated SLE phase diagrams according to the different sets of parameters used to represent the behaviors. The phase diagram with the lowest deviation in each case is represented in the bottom right of the figure.

Both the approaches improved the accuracy of the theoretical *liquidus* line and, consequently the description of the *solidus* line when compared to the previous one-variable problem. The observed minimum deviations (eqn (14)) were described by valleys and not single points. However, the area of valleys decreased with the increasing of the accuracy of the model to represent the activity coefficients and the quality and quantity of experimental data. In the first case, sketched in Fig. 12, an adjustable equation was introduced for the calculation of the activity coefficients of both the phases. In the second case,
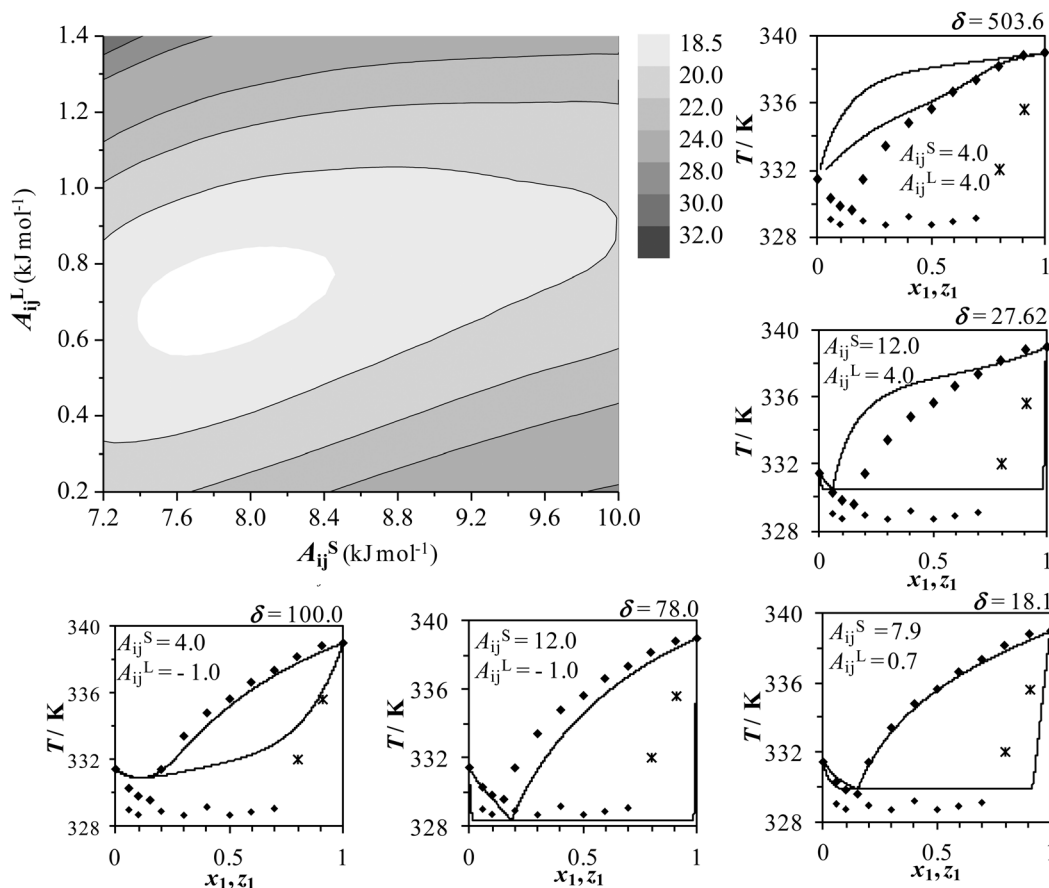
This journal is © the Owner Societies 2014

Phys. Chem. Chem. Phys., 2014, **16**, 16740–16754 | **16749**

Fig. 12 Deviations δ (eqn (14)) from experimental data for the system tripalmitin + octadecanol using the 2-suffix Margules equation as γ_i^L and γ_i^S models. A_{ij}^S and A_{ij}^L are the γ_i^S and γ_i^L parameters (kJ mol^{-1}), respectively. In detail, phase diagrams using different parameters sets.

sketched in Fig. 13, an equation with two parameters was used for calculating solid phase activity coefficients while keeping the predictive character of the liquid phase activity coefficients. In general, the second approach, *i.e.* using the 3-suffix Margules as the γ_i^S equation and the original UNIFAC as the γ_i^L equation, more precisely described the phase diagrams. The mean deviation decreased from δ = (18.10 to 3.0), approximately, especially because of the better characterization of the *solidus* line. In fact, the calculation of the non-ideality of the compounds by the 2-suffix Margules equation is such that the behavior is strictly symmetrical reflecting the specific feature of this model (eqn (2)). Symmetrical activity coefficient values show that the compounds have similar mutual interactions. However, such an assumption is probably not the best in the present cases. In fact, using the non-symmetrical 3-suffix Margules equation the activity coefficients values assume very distinguished behaviors.

Fig. 14 sketches the results obtained by applying the 3-suffix Margules equation for the description of the non-ideality of both liquid and solid phases. The optimization of this method considered a four-directional search. In this case, similar to the previous cases, a cross-evaluation of two matrices $A_{ij}^S \times B_{ij}^S$ (parameters for γ_i^S equation) and $A_{ij}^L \times B_{ij}^L$ (parameters for γ_i^L equation) were performed, and the region with the lowest deviations was depicted. The first contour plot $A_{ij}^S \times B_{ij}^S$ presents

the results at a fixed set of γ_i^L parameters (A_{ij}^L, B_{ij}^L) and the second one $A_{ij}^L \times B_{ij}^L$ at a fixed set of γ_i^S parameters (A_{ij}^S, B_{ij}^S). The fixed parameters were inside the best fitting region observed. The adjustment was considerably improved with deviations (eqn (14)) lower than δ = 1.6. With this improvement one can expect that the behavior of activity coefficients was more precisely assessed. In the last cases, the liquid phase activity coefficients were very close to ideality, presenting positive or negative deviations not higher than 10%. However, by this approach, the deviation from ideality of the liquid phase presented marked negative deviations of up to 25%. In fact, Fig. 11 showed that by considering the liquid phase as ideal the *liquidus* line presented a slight negative deviation. Similarly, the positive non-ideality of the solid phase was slightly decreased when compared with the last cases. It implies that the improvement of the description of the liquid phase non-ideality, and consequently the *liquidus* line, improved the non-ideal profile of the solid phase. Thus, the *solidus* line was also more precisely assessed.

Moreover, in this last case, the activity coefficient values of the triacylglycerol in the solid phase varied from a positive deviation at low concentrations to a significant negative deviation (up to 10%) at high concentrations. This is very interesting taking into account the formation of a solid solution observed at high concentrations of TAGs. It implies that at low concentrations
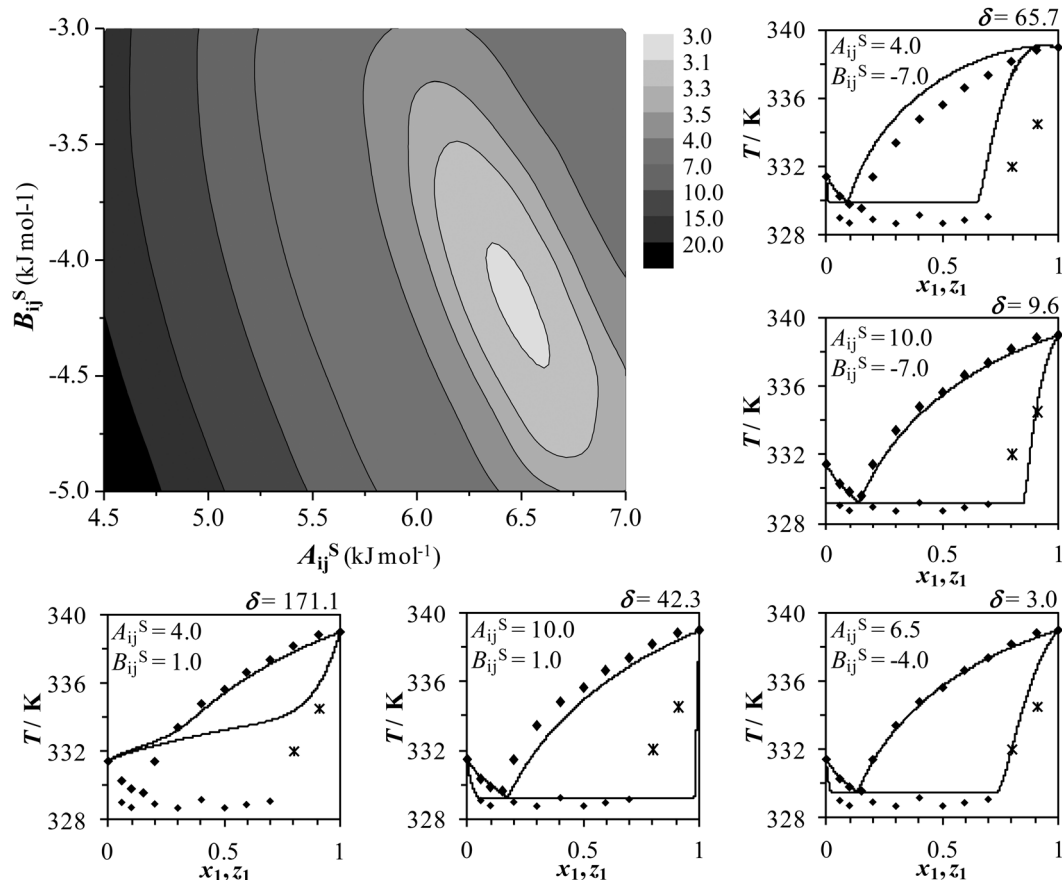
Fig. 13 Deviations δ (eqn (14)) from experimental data for the system tripalmitin + 1-octadecanol using the original UNIFAC as γ_i^{L} model and the 3-suffix Margules equation as γ_i^{S} model with A_{ij}^{S} and B_{ij}^{S} as parameters. In detail, phase diagrams using different parameter sets.

of TAGs the tendency of the compounds in the solid phase is to be independently crystallized because positive deviations show unfavourable interactions. However, at high concentrations of TAGs, because of the favourable interactions in the solid phase, represented by the negative deviations of the TAGs, one might confirm that, in fact, the crystalline structure of the TAG could probably act as a host for the crystalline structure of the fatty alcohol such that the solid solution is the most favourable equilibrium condition. In addition, it was observed that the higher the triacylglycerol carbon chain, the larger the solid solution region. This is in agreement with the activity coefficient values because the decrease of the TAG carbon-chain led to an increase in the deviation value. This means implies in these cases the tendency of the compounds in the solid phase to be independently crystallized is higher than the tendency of formation of the solid solution.

Fig. 12 to 14 also show, in detail, the evolution of the behavior of the phase diagram shape using different parameter sets. This is interesting because the parameters of the γ_i equations were directly related to the non-ideality of the system. In general, when the parameters of both liquid and solid phase γ_i equations were low, the trend to an ideal behavior ($\gamma_i \rightarrow 1$) increased and consequently the trend to show a continuous solid solution SLE phase diagram also increased.

Increasing the values of the solid phase γ_i equation parameters led to an increase in the positive deviation from ideality and consequently to the solid–solid phase separation. The behavior of the *liquidus* and *solidus* lines thus showed a discontinuity, corresponding to the eutectic point. The higher the positive deviation in γ_i^{S} values the smaller the solid solution region until the compounds were completely immiscible in the solid phase.

As mentioned before, by using the heuristic method the optimized answer was a region and not a single set of parameters. It implies that in the minimum deviation region, the set of parameters float around a small range of values. This implies that once the *liquidus* line is accurately predicted by a defined set of parameters, the modeling can fail in the description of the *solidus* line. Similarly, when a set of parameters are used for the accurate description of the *solidus* line, the behavior of the *liquidus* line is slightly altered. Thus, the minimum region assumes a rough surface-type shape which prevented the utilization of an optimization procedure based on a classical numerical method.

Modeling results for all the binary mixtures experimentally evaluated in this work are depicted in Fig. 5 and, as indicated, the 3-suffix Margules equation was considered for the calculation of non-ideality of both the liquid and solid phases. Quantitatively, this approach provided the best description of
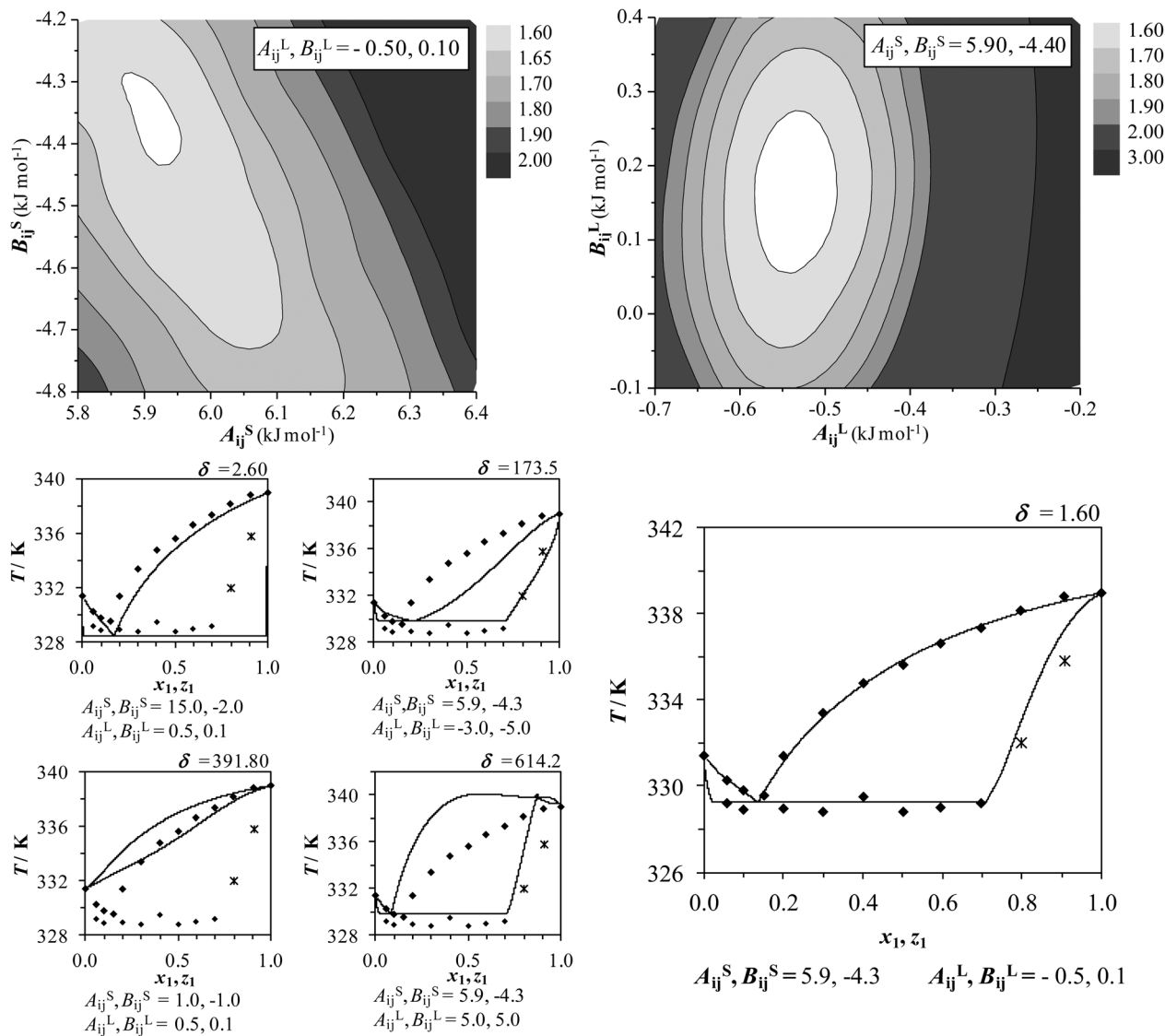
This journal is © the Owner Societies 2014

Phys. Chem. Chem. Phys., 2014, **16**, 16740–16754 | **16751**

Fig. 14 Deviations δ (eqn (14)) from experimental data for the system tripalmitin + 1-octadecanol using the 3-suffix Margules equation as both γ_i^L and γ_i^S models. A_{ij}^S and B_{ij}^S are parameters for γ_i^S and A_{ij}^L and B_{ij}^L are parameters for γ_i^L. In detail, phase diagrams using different parameter sets.

the SLE behavior with the lowest deviations between the calculated and experimental data. In fact, when compared with other approaches, the increase in the accuracy was in this case obtained by the increase of the number of adjustable parameters. However, this implied the decrease in the predictive ability of the model. Qualitatively, the utilization of the UNIFAC model as the γ_i^L equation and the 3-suffix Margules equation for the solid phase also presented reasonable results. Even with slightly higher deviations, this approach presented a higher predictive ability and was also able to represent the overall thermodynamic behavior of the mixtures.

Conclusions

The non-ideality of the solid phase could be embodied in the SLE modeling by an effective procedure called the *Crystal-T* algorithm. In contrast with previously reported studies that

usually consider lipidic mixtures to exhibit a solid phase with independently crystallized compounds independently, triacylglycerol + fatty alcohol systems presented a discontinuous solid solution behavior. In this manner, the *Crystal-T* algorithm was able to accurately depict the solid solution region, neglected by usual theoretical approaches in literature. For this, the routine used the experimental composition in the triphasic equilibrium condition (SSLE) obtained by the Tammann plots of the eutectic transition. Moreover, when compared with the Gibbs and *flash* algorithms, the *Crystal-T* algorithm was found not to be sensitive to initial estimates and thus very robust and effective. This is because it calculates SLE from a given liquid phase x_i, which is a composition of the *liquidus* line, from $x_1 = 0$ to 1 and from $x_1 = 1$ to 0. In addition, the algorithm avoids the problem with the discontinuity of the function in the eutectic point, and additional routines to test the number of phases, classically used in the Gibbs and *flash* SLE algorithms.

16752 | *Phys. Chem. Chem. Phys.*, 2014, **16**, 16740–16754

This journal is © the Owner Societies 2014

The most accurate results were obtained by the 3-suffix Margules equation for describing both the *liquidus* and *solidus* lines because of the increase in the number of adjustable parameters. However, considering the future evaluation of a large set of binary mixtures, and consequently, the construction of a parameters databank, the SLE of more complex systems could be effectively described. Otherwise, considering a reasonable qualitative overall description, the utilization of the original UNIFAC model as γ_i^L associated with the 3-suffix Margules equation as γ_i^S should also be applied.

This work contributed to the expansion of the boundaries of the classical SLE modelling not comprising trivial mixtures as in the case of the food, oil chemistry and pharmaceutical fields.

Acknowledgements

Notes and references

1 R. E. Timms, *Prog. Lipid Res.*, 1984, **23**, 1.
2 L. H. Wesdorp, PhD thesis, Delft University of Technology, 1990.
3 L. Ventola, T. Calvet, M. A. Cuevas-Diarte, X. Solans, D. Mondieig, P. Negrier and J. C. van Miltenburg, *Phys. Chem. Chem. Phys.*, 2003, **5**, 947.
4 L. Ventola, T. Calvet, M. A. Cuevas-Diarte, H. A. J. Oonk and D. Mondieig, *Phys. Chem. Chem. Phys.*, 2004, **6**, 3726.
5 J. A. Gonzalez and U. Domanska, *Phys. Chem. Chem. Phys.*, 2001, **3**, 1034.
6 L. Ventola, T. Calvet, M. A. Cuevas-Diarte, D. Mondieig and H. A. J. Oonk, *Phys. Chem. Chem. Phys.*, 2002, **4**, 1953.
7 L. Ventola, T. Calvet, M. A. Cuevas-Diarte, M. Ramirez, H. A. J. Oonk, D. Mondieig and P. Negrier, *Phys. Chem. Chem. Phys.*, 2004, **6**, 1786.
8 IUPAC, *Compendium of Chemical Terminology*, Blackwell Scientific Publications, Oxford, 2 edn, 1997.
9 A. G. Marangoni and S. S. Narine, *Food Res. Int.*, 2002, **35**, 957.
10 A. G. Marangoni, N. Acevedo, F. Maleky, E. Co, F. Peyronel, G. Mazzanti, B. Quinn and D. Pink, *Soft Matter*, 2012, **8**, 1275.
11 F. G. Gandolfo, A. Bot and E. Flöter, *Thermochim. Acta*, 2003, **404**, 9.
12 M. Pernetti, K. F. van Malssen, E. Flöter and A. Bot, *Curr. Opin. Colloid Interface Sci.*, 2007, **12**, 221.
13 A. Bot, Y. S. J. Veldhuizen, R. den Adel and E. C. Roijers, *Food Hydrocolloids*, 2009, **23**, 1184.
14 J. Daniel and R. Rajasekharan, *J. Am. Oil Chem. Soc.*, 2003, **80**, 417.
15 L. Dassanayake, D. Kodali, S. Ueno and K. Sato, *J. Am. Oil Chem. Soc.*, 2009, **86**, 1163.
16 R. R. Egan, G. W. Earl and J. Ackerman, *J. Am. Oil Chem. Soc.*, 1984, **61**, 324.
17 H. M. Schaink, K. F. van Malssen, S. Morgado-Alves, D. Kalnin and E. van der Linden, *Food Res. Int.*, 2007, **40**, 1185.
18 K. W. Won, *Fluid Phase Equilib.*, 1993, **82**, 261.
19 M. Santos, G. C. Roux and V. Gerbaud, *J. Am. Oil Chem. Soc.*, 2011, **88**, 223.
20 S. M. Walas, *Phase equilibria in chemical engineering*, Butterworth, Boston, 1985.
21 R. C. Reid, J. M. Prausnitz and B. E. Pouling, *The properties of gases and liquids*, McGraw-Hill, New York, 4th edn, 1987.
22 J. Gmehling, B. Kolbe, M. Kleiber and J. Rarey, *Chemical Thermodynamics for Process Simulation*, Wiley-VHC, Weinheim, 2012.
23 J. M. Prausnitz, R. N. Lichtenthaler and E. G. Azevedo, *Molecular thermodynamics of fluid-phase equilibria*, Prentice-Hall, New Jersey, 1986.
24 A. Fredenslund, R. L. Jones and J. M. Prausnitz, *AIChE J.*, 1975, **21**, 1086.
25 J. G. Gmehling, T. F. Anderson and J. M. Prausnitz, *Ind. Eng. Chem. Fundam.*, 1978, **17**, 269.
26 J. Gmehling, J. D. Li and M. Schiller, *Ind. Eng. Chem. Res.*, 1993, **32**, 178.
27 H. K. Hansen, P. Rasmussen, A. Fredenslund, M. Schiller and J. Gmehling, *Ind. Eng. Chem. Res.*, 1991, **30**, 2352.
28 M. C. Costa, L. A. D. Boros, J. A. P. Coutinho, M. A. Krähenbühl and A. J. A. Meirelles, *Energy Fuels*, 2011, **25**, 3244.
29 L. Boros, M. L. S. Batista, R. V. Vaz, B. R. Figueiredo, V. F. S. Fernandes, M. C. Costa, M. A. Krähenbuühl, A. J. A. Meirelles and J. A. P. Coutinho, *Energy Fuels*, 2009, **23**, 4625.
30 J. A. P. Coutinho, M. Gonçalves, M. J. Pratas, M. L. S. Batista, V. F. S. Fernandes, J. Pauly and J. L. Daridon, *Energy Fuels*, 2010, **24**, 2667.
31 A. A. Nyqvist-Mayer, A. F. Brodin and S. G. Frank, *J. Pharm. Sci.*, 1986, **75**, 365.
32 P. W. Stott, A. C. Williams and B. W. Barry, *J. Controlled Release*, 1998, **50**, 297.
33 R. Gautam and W. D. Seider, *AIChE J.*, 1979, **25**, 991.
34 H. H. Rachford and J. D. Rice, *Trans. Am. Inst. Min. Metall. Eng.*, 1952, **195**, 327.
35 T. F. Anderson, D. S. Abrams and E. A. Grens, *AIChE J.*, 1978, **24**, 20.
36 G. J. Maximo, M. C. Costa and A. J. A. Meirelles, *Braz. J. Chem. Eng.*, 2013, **30**, 33.
37 G. G. Chernik, *J. Colloid Interface Sci.*, 1991, **141**, 400.
38 M. C. Costa, M. P. Rolemberg, L. A. D. Boros, M. A. Krähenbühl, M. G. de Oliveira and A. J. A. Meirelles, *J. Chem. Eng. Data*, 2007, **52**, 30.
39 L. Ventolà, M. Ramírez, T. Calvet, X. Solans, M. A. Cuevas-Diarte, P. Negrier, D. Mondieig, J. C. van Miltenburg and H. A. J. Oonk, *Chem. Mater.*, 2002, **14**, 508.

40 C. Mosselman, J. Mourik and H. Dekker, *J. Chem. Thermodyn.*, 1974, **6**, 477.

41 N. D. D. Carareto, M. C. Costa and A. J. A. Meirelles, *presented in part at the VI Congresso Brasileiro de Termodinâmica Aplicada*, Salvador, 2011.

42 G. Charbonnet and W. S. Singleton, *J. Am. Oil Chem. Soc.*, 1947, **24**, 140.

43 D. G. Kolp and E. S. Lutton, *J. Am. Chem. Soc.*, 1951, **73**, 5593.

44 U. Domanska and J. A. Gonzalez, *Fluid Phase Equilib.*, 1996, **123**, 167.

45 E. S. Domalski and E. D. Hearing, *J. Phys. Chem. Ref. Data*, 1996, **25**, 1.

46 J. Xing, Z. C. Tan, Q. Shi, B. Tong, S. X. Wang and Y. S. Li, *J. Therm. Anal. Calorim.*, 2008, **92**, 375.

47 G. Nichols, S. Kweskin, M. Frericks, S. Reiter, G. Wang, J. Orf, B. Carvallo, D. Hillesheim and J. Chickos, *J. Chem. Eng. Data*, 2006, **51**, 475.

48 N. Garti, J. Schlichter and S. Sarig, *Fat Sci. Technol.*, 1988, **90**, 295.

49 M. Kellens, W. Meeussen and H. Reynaers, *Chem. Phys. Lipids*, 1990, **55**, 163.

50 M. C. Costa, L. A. D. Boros, J. A. Souza, M. P. Rolemberg, M. A. Krähenbühl and A. J. A. Meirelles, *J. Chem. Eng. Data*, 2011, **56**, 3277.

51 M. C. Costa, L. A. D. Boros, M. P. Rolemberg, M. A. Krähenbühl and A. J. A. Meirelles, *J. Chem. Eng. Data*, 2010, **55**, 974.

52 G. J. Maximo, N. D. D. Carareto, M. C. Costa, A. O. dos Santos, L. P. Cardoso, M. A. Krähenbühl and A. J. A. Meirelles, *Fluid Phase Equilib.*, 2014, **366**, 88.

53 G. F. Hirata, C. R. A. Abreu, L. C. B. A. Bessa, M. C. Ferreira, E. A. C. Batista and A. J. A. Meirelles, *Fluid Phase Equilib.*, 2013, **360**, 379.

54 P. C. Belting, J. Rarey, J. Gmehling, R. Ceriani, O. Chiavone-Filho and A. J. A. Meirelles, *Fluid Phase Equilib.*, 2014, **361**, 215.